

Thermal lens scanning of the glass transition in polymers

J. H. Rohling, A. M. F. Caldeira, J. R. D. Pereira, A. N. Medina, A. C. Bento et al.

Citation: *J. Appl. Phys.* **89**, 2220 (2001); doi: 10.1063/1.1333737

View online: <http://dx.doi.org/10.1063/1.1333737>

View Table of Contents: <http://jap.aip.org/resource/1/JAPIAU/v89/i4>

Published by the [American Institute of Physics](#).

Additional information on J. Appl. Phys.

Journal Homepage: <http://jap.aip.org/>

Journal Information: http://jap.aip.org/about/about_the_journal

Top downloads: http://jap.aip.org/features/most_downloaded

Information for Authors: <http://jap.aip.org/authors>

ADVERTISEMENT



AIP Advances

Now Indexed in
Thomson Reuters
Databases

Explore AIP's open access journal:

- Rapid publication
- Article-level metrics
- Post-publication rating and commenting

Thermal lens scanning of the glass transition in polymers

J. H. Rohling, A. M. F. Caldeira, J. R. D. Pereira, A. N. Medina, A. C. Bento, M. L. Baesso,^{a)} and L. C. M. Miranda

Departamento de Física, Universidade Estadual de Maringá, Av. Colombo 5790, 87020-900, Maringá, PR, Brazil

A. F. Rubira

Departamento de Química, Universidade Estadual de Maringá, Av. Colombo 5790, 87020-900, Maringá, PR, Brazil

(Received 31 July 2000; accepted for publication 23 October 2000)

In this article we discuss the use of the thermal lens technique for investigating the thermal properties of polymers as a function of temperature. It is also discussed how the experimentally determined thermal lens parameters can be used to locate the glass transition in polymers. The methodology is tested using a solution casted films of poly(vinyl chloride) as a testing sample. A comparison with conventional differential scanning calorimetry data is made. It is proposed that the current transient thermal lens methodology, with minor changes in its experimental configuration, could be adapted to develop a new methodology called differential thermal lens scanning especially designed for the investigation of the phase transitions in polymers. It is shown that this new methodology could be equally used for the measurement of the thermal expansion coefficient, above and below the glass transition. © 2001 American Institute of Physics. [DOI: 10.1063/1.1333737]

I. INTRODUCTION

In the last two decades we have witnessed the development of a number of techniques for nondestructive characterization of the thermal, optical, and structural properties of materials based upon the so-called photothermal techniques.¹⁻⁵ The photothermal techniques are essentially based upon sensing the temperature fluctuation of a given sample due to nonradiative deexcitation processes following the absorption of modulated or pulsed light. Apart from having been extensively used in the optical and thermal characterization of a wide spectrum of materials, ranging from semiconductors⁶ to glasses^{7,8} and biological specimens,^{9,10} a growing number of applications of these photothermal techniques have been used for investigating the different physicochemical properties of polymers,¹¹⁻¹³ as well as how the processing conditions¹⁴⁻¹⁷ of these materials affect their physical properties. Despite this growing interest and the importance of the applications of these techniques to the polymer research area, so far the photothermal measurements have been carried out mostly at near room-temperature conditions. This apparent limitation is essentially dictated by the fact that most of the photothermal polymer measurements reported so far were based upon the use of the photoacoustic technique. In a conventional photoacoustic experimental setup, the sample is enclosed in an airtight cell and exposed to a chopped light beam. As a result of the periodic heating of the sample due to light absorption, the air pressure inside the cell oscillates at the chopping frequency and is detected by a sensitive microphone coupled to one of the cell's walls.

The use of an electret microphone is the main reason why applications to polymers have been restricted to near room temperatures.

In this article we discuss the use of an alternative photothermal technique for measurements of the thermal properties of polymers as a function of temperature. The proposed technique is based upon the use of the thermal lens (TL) technique.¹⁸⁻²⁰ The thermal lens effect was first observed by Gordon *et al.*,¹⁸ and it consists basically on the observation of the changes induced in the refractive index of a sample as it is heated by an incident laser beam. The energy absorbed by the sample is converted, in part or in whole, into heat by nonradiative deexcitation processes. The temperature disturbance thus creates a spatially dependent change in the refractive index n of the sample. This spatially dependent refractive index turns the light beam propagation region within the sample into a lens-like medium for the light beam. In the cases where $\partial n/\partial T$ is negative, as in most liquids and gases, the thermal lens is a diverging lens, whereas when $\partial n/\partial T$ is positive one has a beam focusing. Thus by measuring the resulting spreading or focusing of an incident laser beam one can evaluate the thermo-optical properties of the sample. The room-temperature thermal lens technique has proven to be a valuable method for investigating not only the complete thermal and spectroscopic properties of transparent materials,²¹⁻²⁴ such as glasses and polymers, but also for the sensitive monitoring of the kinetics of fast chemical reactions,²⁵ percolation in microemulsions,²⁶ and dynamics of water-surfactant interaction.²⁷ Since the thermal lens technique is an intrinsically remote technique the measurements on a sample placed inside a harsh environ-

^{a)} Author to whom correspondence should be addressed. Electronic mail: mlbaesso@uem.br

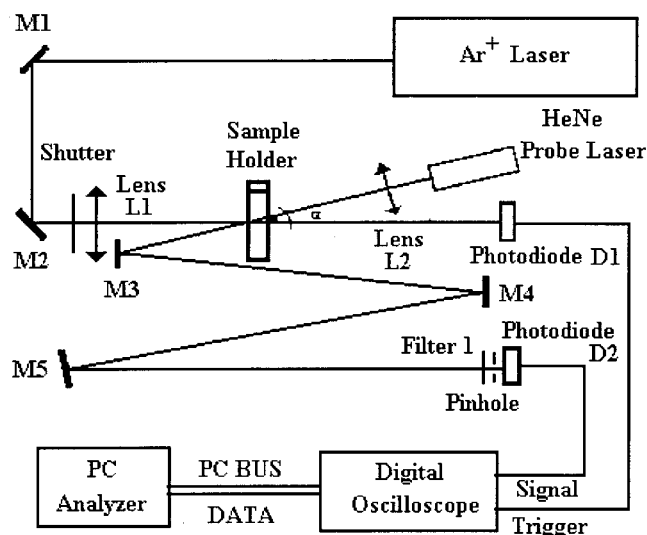


FIG. 1. Two-beam mode mismatched experimental configuration.

ment presents, in principle, no extra difficulty.^{28–30} It is precisely this aspect we take advantage of to carry on the thermal properties measurements of polymers as a function of temperature.

II. EXPERIMENT

There are several experimental configurations for the thermal lens spectroscopy. Of these, the two-beam mode mismatched experimental configuration has been shown^{31–33} to be the most sensitive one. Accordingly, we have resorted to this configuration for our temperature dependent thermal lens measurements. The mode-mismatched thermal lens experimental setup is schematically shown in Fig. 1. An Ar⁺ laser (Coherent Innova 90 Plus) operating at 514.5 nm is used as the excitation pumping beam and a He–Ne laser as the probe beam. The sample is positioned at the waist of the excitation laser beam, where the power density is maximum. The excitation beam was focused with a $f_1 = 25$ cm lens (L_1), and the sample was positioned at its focal plane. The sample exposure to the excitation beam is controlled by a shutter. The probe beam was focused using a converging lens (L_2) with focal length $f_2 = 15$ cm at an angle $\alpha < 1.5^\circ$ with respect to the excitation beam and centered in order to maximize the thermal lens signal. The probe and excitation beam radius at the sample were 153 and 53.5 μm , respectively. The excitation beam was incident on a detector (D_1) which was used for triggering. The adjustable mirrors M_3 , M_4 , and M_5 were employed to produce a long optical path (≈ 2 m) from the sample to an iris mounted in front of detector (D_2). The output signals from the triggering detector and the probe beam detector were fed into a digital oscilloscope. All data acquisition was microcomputer controlled. In all experiments the thermal lens signals were recorded during approximately 30 ms. The sample optical absorption coefficient at the pumping beam wavelength was determined by measuring the Ar⁺ laser transmitted power at

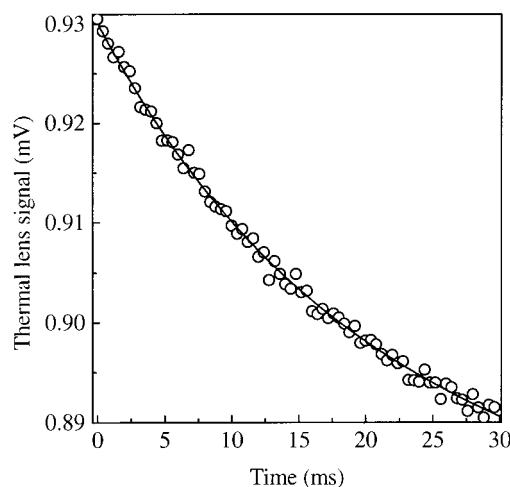


FIG. 2. Typical transient TL signal for the PVC sample for a pumping beam power of 75 mW at room temperature. The solid line corresponds to the data fitting to Eq. (1) leaving θ and t_c as adjustable parameters. The values obtained were $\theta = (0.0791 \pm 0.0009)$ and $t_c = (5.50 \pm 0.06)$ ms.

detector D_1 , as a function of the incident power, using the same experimental configuration without the simultaneous He–Ne laser illumination.

The testing sample used in this work consisted of 200 μm thick 12 mm diameter disks of poly (vinyl chloride) (PVC) films. The PVC films were prepared using a 20 000 molar weight PVC powder (Aldrich). The films were cast from a 6.5% (w/w) 1,2-dichloroethane solution at room temperature over a flat clean glass substrate. For the thermal lens experiments the samples were removed from the substrate and placed inside a temperature-controlled minioven with a hole in its center allowing the access of the laser beams. Finally, in order to validate and evaluate the sensitivity of the proposed method we have also carried complementary measurements of the samples specific heat, using the transient heat method,³⁴ and differential scanning calorimetry (DSC) for the evaluation of the glass transition temperature.

III. RESULTS AND DISCUSSION

In Fig. 2 we show a typical transient TL signal for the PVC sample for a pumping beam power of 75 mW at room temperature. The solid lines in Fig. 2 correspond to the data fitting to the theoretical curve. The mode-mismatched TL configuration theory is treated in details in Refs. 22, 32, and 33. In the derivation of the model, which considers the aberrant nature of the thermal lens effect, the following assumptions have been made: the excitation and probe beams are TEM₀₀ and Gaussian; the sample should satisfy the Beer's law; the detection of the intensity of the distribution of the probe beam in the detector is undertaken in the Fresnel region; and finally, in order to have the same temperature rise distribution in the direction of the laser propagation, the sample thickness should be shorter than the confocal distance of both the excitation and probe beams. This model may be summarized as follows. As a result of the pumping beam absorption by the sample, a local temperature rise is

produced within the sample. The change of the sample refractive index with the temperature produces a lens-like element within the heated region. A weak probe beam propagating through this heated region will experience an optical path length change, resulting, in turn, in a variation of its intensity at the beam center. The resulting change of the center probe beam intensity, $I(t)$, due to the TL effect can be expressed as

$$I(t) = I(0) \left\{ 1 - \frac{\theta}{2} \times \tan^{-1} \left[\frac{2mV}{1 + 2m + V^2 + [(1 + 2m)^2 + V^2](t_c/2t)} \right] \right\}^2, \quad (1)$$

where

$$m = \left(\frac{\omega_{1p}}{\omega_e} \right)^2, \quad V = \frac{z_1}{z_c}, \quad z_1 \ll z_2, \quad t_c = \frac{\omega_e^2}{4D}. \quad (2)$$

Here t_c is the characteristic thermal lens time constant, ω_e is the excitation laser beam radius at the sample, defined as the radius for which field amplitude in the Gaussian beam has fallen to e^{-1} of its axial value, $D = k/\rho c$ is the sample thermal diffusivity, ρ its mass density, c the sample specific heat, and k its thermal conductivity. The parameter z_c is the confocal distance of the probe beam, z_1 is the distance between the probe beam waist and the sample, z_2 is the distance between the sample and the detector, ω_{1p} is the probe beam radius at the sample, and $I(0)$ is the value of the probe beam intensity at $t=0$. The TL transient signal amplitude parameter θ in Eq. (1) is given by²²

$$\theta = - \frac{PAL}{k\lambda_p} \frac{ds}{dT} \quad \text{with } L \ll Z_c. \quad (3)$$

The parameter θ is approximately equal to the phase difference of the probe beam at $r=0$ and $r=\omega_e\sqrt{2}$ induced by the thermal lens. P is the excitation beam power, A is the sample absorption coefficient at the excitation beam wavelength, λ_p is the probe beam wavelength, and ds/dT is the temperature coefficient of the optical path length given by

$$\frac{ds}{dT} = (n-1) \frac{1}{L} \left(\frac{dL}{dT} \right)_{T_0} + \left(\frac{dn}{dT} \right)_{T_0}, \quad (4)$$

where n and L are the sample refractive index and thickness, respectively, at the initial temperature T_0 . The above expression for ds/dT involves both sample dilatation and refractive index changes with temperature. According to Refs. 22 and 35 it can be rewritten as

$$\frac{ds}{dT} = (n-1)(1+\nu)\alpha_T + \frac{dn}{dT}, \quad (5)$$

where α_T is the sample linear thermal expansion coefficient, ν its Poisson ratio, and dn/dT is the temperature coefficient of its refractive index. Equation (5) can be further simplified if one uses the Clausius–Mossotti relation to calculate dn/dT . One gets:²²

$$\frac{ds}{dT} = - \left(\frac{n-1}{6n} \right) \{ [(n+1)(n^2+2) - 2n(1+\nu)] 3\alpha_T - (n+1)(n^2+2)\phi \}, \quad (6)$$

where ϕ is the polarizability temperature coefficient. We note that in Eqs. (1) and (2) the parameters z_c , ω_e , and ω_{1p} are determined by spot size measurements, whereas the parameters z_1 and z_2 are determined by the experimental geometry. We are thus left with only two unknown parameters, namely, θ and t_c which can be determined from the time-resolved TL signal data fitting. Knowing θ and t_c , we can readily find both ds/dT and the thermal diffusivity D . The values of the laser beam profiles and the geometric parameters used in the current TL experiments were $\omega_e = (5.35 \pm 0.02) \times 10^{-3}$ cm, $\omega_{1p} = (15.29 \pm 0.06) \times 10^{-3}$ cm, $z_c = (2.78 \pm 0.02)$ cm, $z_1 = (4.94 \pm 0.02)$ cm, $m = (8.17 \pm 0.07)$, and $\nu = (1.78 \pm 0.04)$.

The solid curve in Fig. 2 corresponds to the data fitting to Eq. (1) leaving θ and t_c as adjustable parameters. For the room-temperature PVC sample data shown in Fig. 2, the values we got from the data fitting were $\theta = (0.0791 \pm 0.0009)$ and $t_c = (5.50 \pm 0.06)$ ms. The corresponding value of the thermal diffusivity, obtained from the characteristic time t_c , was $D = (1.29 \pm 0.03) \times 10^{-3}$ cm²/s. In particular, we note that the value we have found for the PVC thermal diffusivity at room temperature agrees quite well with those reported in the literature,³⁶ namely, 1.2×10^{-3} cm²/s. The same procedure was carried out at the different temperatures of interest up to 70 °C. For each temperature adjusted in the oven, the experiments were done at seven different excitation laser powers. We remind the reader that in the thermal lens experiment a change in the refractive index from the beam center to the beam edge necessary to obtain a detectable signal requires a very small temperature change of the order of 10^{-2} to 10^{-3} °C,¹⁸ which can be considered insignificant as compared to the minimal scanning step used (0.1 °C) in this study. Finally, comparing Eqs. (3) and (6), we note that the fact that the value we have found for θ is positive means that the thermal expansion component of ds/dT in Eq. (6) dominates over the polarizability contribution.

In Figs. 3 and 4 we show the resulting temperature dependence we got for the thermal diffusivity and the normalized thermal lens signal parameter θ of our PVC samples, respectively. Now the TL measurements give us only the values of D and θ so that additional measurements of the specific heat and mass density are needed in order to obtain the thermal conductivity k . We remember that k is related to D by $k = \rho c D$. The specific heat of our PVC samples were measured using a homemade calorimeter based on the transient heat method.³⁴ As to the temperature dependence of the PVC mass density we have used the literature values.³⁶ Using the measured values of c and D together with the tabulated values of ρ , we have calculated the thermal conductivity k . In Fig. 5 we show the resulting temperature dependence of both c and k . At room temperature, the value we got for k was (1.87 ± 0.03) mW/cm K, which is close to the value reported in the literature,³⁶ namely, 1.6 mW/cm K. The solid line in the plot of c represents the smoothing of the

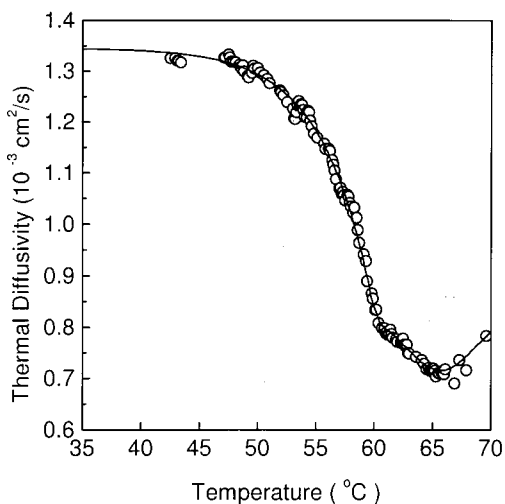


FIG. 3. Thermal diffusivity of the 200 μm thick PVC films as a function of temperature. The solid line represents the result of the experimental data fitting to two Lorentzians.

experimental data, whereas in the plot of k the solid line is the product of the smoothed data for ρ , c , and D . From the values of θ/P and k , together with the known³⁶ room-temperature values of $n = 1.546$, $dn/dT = -1.14 \cdot 10^{-4} \text{ K}^{-1}$, and $\nu = 0.38$, one can estimate the room-temperature thermal expansion coefficient α_T from Eqs. (3) and (5). We got $\alpha_T = 6.9 \times 10^{-5} \text{ K}^{-1}$, which is in very good agreement with the one reported in the literature.³⁶

The behavior of the thermal conductivity of amorphous solids presents considerable difficulties due to the absence of long-range order in these systems. For example, the available experimental data indicate that in contrast to the thermal conductivity of crystalline bodies, the thermal conductivity of amorphous solids has no low-temperature maximum, and, as a rule it increases with a rise in temperature. In the case of amorphous polymers, the typical feature³⁷ is that up to the glass transition temperature the thermal conductivity increases with a rise in temperature and above T_g it begins to

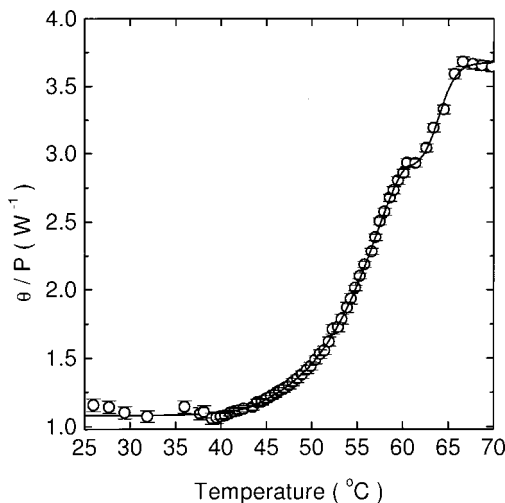


FIG. 4. Thermal lens normalized signal amplitude parameter θ of 200 μm thick PVC films as a function of temperature. The solid line represents the fitting of the experimental data.

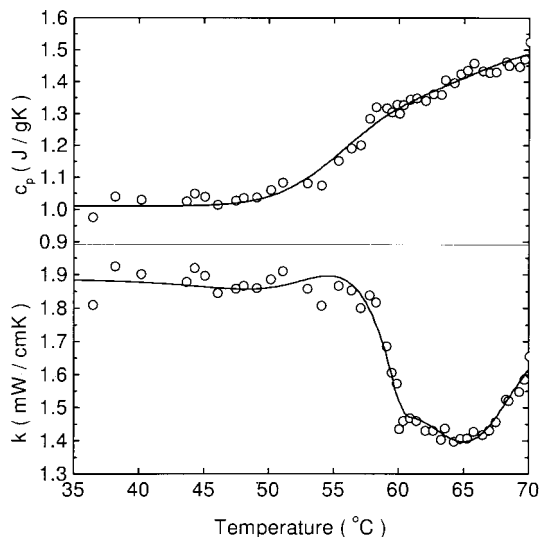


FIG. 5. Temperature dependence of the specific heat and thermal conductivity of our PVC films. The solid lines represent the smoothed experimental data.

decrease. This behavior of k near T_g has been explained by Eierman.^{38,39} His reasoning is based on Debye's model for the thermal conductivity in which k is given by

$$k = \frac{1}{3} \rho c \bar{v}_s l, \tag{7}$$

where \bar{v}_s is the average sound velocity and l is the phonon mean free path. Eierman assumed that the mean free path in amorphous substances coincides, in a first approximation, with the mean distance between two neighboring atoms, and wrote the average sound velocity as $\sqrt{K/M}$ where K is the elastic constant characterizing the bonding force between two neighboring atoms with masses M_1 and M_2 , with m equal to $(M_1 + M_2)/2$. Making these substitutions into the Debye's expression it follows that the thermal conductivity essentially scales with $\sqrt{K/M}$. Accordingly, one should then expect that above T_g the thermal conductivity should decrease due to the decrease of the elastic constant caused by the intermolecular interaction. In our case the decrease of the thermal conductivity observed in Fig. 5 occurs at roughly 55 $^\circ\text{C}$. Furthermore, above 65 $^\circ\text{C}$, the thermal conductivity data shown in Fig. 5 exhibited an increase with increasing temperature. This behavior in the fluid phase is in agreement with the general feature of the temperature dependence of the thermal conductivity of an amorphous material, for which K increases with a rise in temperature, as mentioned above. Finally, we note that the data shown in Fig. 3 for the thermal diffusivity is also in close agreement with the predictions of Debye's model. According to this model the thermal diffusivity is related to the average sound velocity by $D = \bar{v}_s l/3$. Thus the features of the D as a function of temperature are essentially reflecting the corresponding changes in the sound velocity. The results of numerous experimental investigations⁴⁰ carried out at low and high frequencies have shown that the sound velocity in polymers depends linearly on temperature and that only at those points where the mode of molecular motion is changed does the temperature coefficient of the sound velocity change discontinuously. Thus the

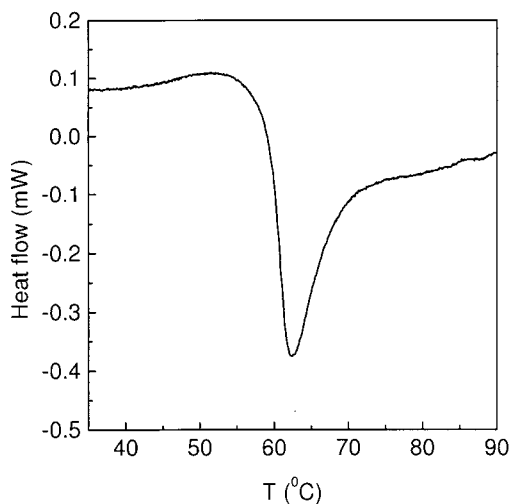


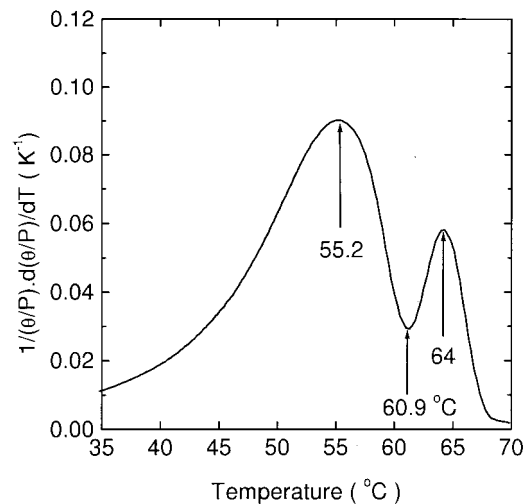
FIG. 6. Differential scanning calorimetry of our PVC sample.

unfreezing of one or another type of molecular motion can be accessed from the kink in the temperature dependence of the sound velocity. The temperature dependence of the thermal diffusivity shown in Fig. 3 is clearly exhibiting this feature. The temperature at which one observes the sharp change in the slope of D occurs at roughly 55°C in reasonable agreement with the T_g value found from the thermal conductivity data. In Fig. 6 we present a typical differential scanning calorimetry (DSC) curve for our PVC samples. This result indicates that the glass transition region of our PVC samples extends from 58°C to roughly 67°C with a peak at $T_g = 62.5^\circ\text{C}$, in agreement with the marked changes of both D and θ/P in this temperature range as shown in Figs. 3 and 4.

To get further insights into the observed temperature dependences, as well as to understand how the thermal lens measurements may be used for analyzing glass transition in polymers, we have next carried out a best fitting of our data to some sigmoidal type of functions so that the data could be represented by a continuous differentiate curve. In doing so, we first note that the experimental data of both D and θ/P exhibit a marked change of their temperature dependence in the vicinity of 60°C . This is clearly seen, for instance, in Fig. 4 in which around this temperature the curve seems to go through a small saturation followed by a sudden jump on further increasing the temperature. A similar change in the temperature dependence around 60°C is also noted in the thermal diffusivity. Accordingly, we have divided the thermal diffusivity and the θ/P data into two sets, corresponding to temperatures below and above 60°C , and carried out the data fittings on each temperature region separately. For the thermal diffusivity, D , each set was best fitted to a Lorentzian function of the form

$$y = y_0 + \frac{A}{\pi} \frac{w/2}{(x - x_0)^2 + (w/2)^2}. \quad (8)$$

For the normalized TL signal amplitude, θ/P , the data fitting was done using the same type of Lorentzian function for temperatures below 60°C , and a logistic function of the form

FIG. 7. Temperature dependence of the temperature derivative of the thermal lens signal amplitude parameter θ , normalized to the pumping power P , $[1/(\theta/P)]d(\theta/P)/dT$, showing the onset of the glass transition.

$$y = A_2 + \frac{(A_1 - A_2)}{1 + \pi(x/x_0)^\nu} \quad (9)$$

for the data set corresponding to temperatures above 60°C . The solid curve in Figs. 3 and 4 represent the results of these piecewise data fittings.

The somewhat complex temperature dependence of both D and θ/P may be better understood by looking at the temperature derivative of the adjusted data. In Fig. 7 we show the result we got for $[1/(\theta/P)]d(\theta/P)/dT$, as a function of temperature. It tells us that on increasing the temperature $[1/(\theta/P)]d(\theta/P)/dT$ increases, goes through a peak around 56°C , then decreases very sharply to a minimum at roughly 61°C , to finally reach a maximum at 64°C . This plot, which is in close resemblance with that of the DSC shown in Fig. 6, reflects quite well the PVC glass transition. This result is indeed not as surprising as it may look at first glance. In a DSC experiment one has a reference material, the sample to be probed, and a predetermined heating (or, cooling) rate is imposed to the system for undergoing a given temperature excursion. A servosystem makes the sample to follow the temperature of the reference and the heating power difference between the sample and reference is recorded. That is, since dT/dt is fixed, one senses essentially dQ/dT . The similarity between the behavior of $[1/(\theta/P)]d(\theta/P)/dT$ and the DSC curve, as seen from Figs. 6 and 7, suggests that the TL technique can indeed be used to perform an equivalent differential scanning technique, namely, a differential thermal lens scanning, in which we set a given heating rate and measure the rate of change of the thermal lens signal. The resulting signal of this scanning technique would be $d\theta/dt = (d\theta/dT)(dT/dt)$, that is, proportional to $d\theta/dT$, and can, according to the above discussion, provide us information regarding the onset of the glass transition. To explore the potentialities of this scanning technique we look at the behavior of $d\theta/dT$ on temperature.

The temperature derivative of θ , as given by Eq. (3), may be written as

$$\frac{d\theta}{dT} = \theta \left\{ \alpha_T - \frac{1}{k} \left(\frac{dk}{dT} \right) + \frac{1}{ds/dT} \left(\frac{d(ds/dT)}{dT} \right) \right\}. \quad (10)$$

Equation (10) indicates that, knowing the temperature dependence of θ , k , and dn/dT , one cannot only identify the glass transition but also determine the sample's thermal expansion coefficient as a function of temperature.

IV. CONCLUSIONS

In this article we have demonstrated the usefulness of the thermal lens technique for the measurement of the thermal properties of transparent polymers as a function of temperature as well as for the determination of their glass transitions. The transient thermal lens signal data fitting yields two parameters, namely, the thermal lens amplitude parameter θ and the characteristic time constant t_c . From the value of t_c , the thermal diffusivity is straightforwardly obtained. The temperature dependence of both D and θ give us information on the glass transition. The latter, however, is more clearly seen by plotting the temperature derivative of θ as a function of temperature, as demonstrated in Fig. 7.

By exploring the similarity between the temperature dependence of $d\theta/dT$ and the results of conventional DSC measurements we were led to suggest that, with minor changes, the current transient thermal lens technique could be adapted to perform a so-called differential thermal lens scanning for locating the glass transition temperatures in polymers. When complemented with specific heat and refractive index measurements, this thermal lens scanning could also be used to determine the sample's thermal expansion coefficient, above and below the glass transition temperature. The proposed thermal lens scanning would be carried out by setting an adequate heating rate, and recording the transient thermal lens signal every, say, 100 ms. Here we note that a typical thermal lens transient lasts for, say, roughly 50 ms, as can be seen in Fig. 2. Taking these typical numbers, and using a heating rate of the order of 3 K/min one would get an average of 20 thermal lens transients every 0.1 K temperature change. Using the results so obtained for θ , $d\theta/dT$, and D , together with the corresponding values of c , we could then not only locate the glass transition but also calculate the room-temperature thermal expansion coefficient.

As compared to conventional DSC the proposed thermal lens temperature scanning technique requires no reference sample, thereby avoiding the eventual time lapse, and thus a finite time interval, during which the reference continues its temperature excursion while the sample temperature stays behind. In contrast, in the thermal lens scanning the only point to be considered is the adequate choice of the heating rate. This should be such that, at each TL transient shot, thermalization within the sample is ensured. For the specific geometry used in our experiments on PVC, thermalization is reached within a time interval of the order of 60 ms. Furthermore, since the temperature fluctuation within the sample during each TL experiment is of the order of a few mK accurate measurements very close to phase transitions are envisaged. Finally, it should be mentioned that the thermal

lens technique is an intrinsically remote local probe. This aspect suggests the possibility of performing thermal properties homogeneity investigations in a given sample. We believe that the simplicity and the remote character of the thermal lens methodology may render this technique and the proposed thermal scanning as valuable alternative tools for the thermal characterization of a wide range of polymers.

ACKNOWLEDGMENT

We are grateful to the Brazilian agencies Capes and CNPq for the partial support of this work.

- ¹A. Rosencwaig, *Photoacoustics and Photoacoustic Spectroscopy* (Wiley, New York, 1980).
- ²H. Vargas and L. C. M. Miranda, *Phys. Rep.* **161**, 43 (1988).
- ³R. D. Snook, *Analyst* (Cambridge, U.K.) **125**, 45 (1999).
- ⁴R. D. Snook, R. D. Lowe, and M. L. Baesso, *Analyst* (Cambridge, U.K.) **123**, 587 (1998).
- ⁵A. C. Tam, *Rev. Mod. Phys.* **58**, 381 (1986).
- ⁶O. Pessoa, Jr., C. L. Cesar, N. A. Patel, H. Vargas, C. C. Ghizoni, and L. C. M. Miranda, *J. Appl. Phys.* **59**, 1316 (1986).
- ⁷A. M. Mansanares, M. L. Baesso, E. C. da Silva, F. C. G. Gandra, H. Vargas, and L. C. M. Miranda, *Phys. Rev. B* **40**, 7912 (1989).
- ⁸M. L. Baesso, A. M. Mansanares, E. C. da Silva, H. Vargas, and L. C. M. Miranda, *Phys. Rev. B* **40**, 1880 (1989).
- ⁹D. C. Fork and S. K. Herbert, *Photochem. Photobiol.* **57**, 207 (1993).
- ¹⁰W. J. Silva, L. M. Priolli, A. C. N. Magalhaes, A. C. Pereira, H. Vargas, A. M. Mansanares, N. Cella, L. C. M. Miranda, and J. J. Alvarado-Gil, *Plant Sci.* **104**, 177 (1995).
- ¹¹A. Lachaine and P. Poulet, *Appl. Phys. Lett.* **45**, 953 (1984).
- ¹²N. F. Leite, N. Cella, H. Vargas, and L. C. M. Miranda, *J. Appl. Phys.* **61**, 3025 (1987).
- ¹³A. Torres-Filho, L. F. Perondi, and L. C. M. Miranda, *J. Appl. Polym. Sci.* **35**, 103 (1988).
- ¹⁴D. Dadarlat, M. Bicanan, A. Frandas, V. V. Morariu, A. Pasca, H. Jalink, and D. Bicanic, *Instrum. Sci. Technol.* **25**, 235 (1997).
- ¹⁵B. Merté, P. Korpiun, E. Lusher, and R. Tilgner, *J. Phys. Colloq.* **44**, 463 (1983).
- ¹⁶P. Korpiun, B. Merté, R. Tilgner, and E. Lusher, *Colloid Polym. Sci.* **261**, 312 (1983).
- ¹⁷A. H. Franzan, N. F. Leite, and L. C. M. Miranda, *Appl. Phys. A: Solids Surf.* **A50**, 431 (1990).
- ¹⁸J. P. Gordon, R. C. C. Leite, R. S. Moore, S. P. S. Porto, and J. R. Whinnery, *J. Appl. Phys.* **36**, 3 (1965).
- ¹⁹J. R. Whinnery, *Acc. Chem. Res.* **7**, 225 (1974).
- ²⁰S. J. Sheldon, L. V. Knight, and J. M. Thorpe, *Appl. Opt.* **21**, 1663 (1982).
- ²¹M. L. Baesso, J. Shen, and R. D. Snook, *Chem. Phys. Lett.* **197**, 255 (1992).
- ²²M. L. Baesso, J. Shen, and R. D. Snook, *J. Appl. Phys.* **75**, 3732 (1994).
- ²³M. L. Baesso, A. C. Bento, A. R. Duarte, A. M. Neto, and L. C. M. Miranda, *J. Appl. Phys.* **85**, 8112 (1999).
- ²⁴M. L. Baesso, A. C. Bento, A. A. de Andrade, J. A. Sampaio, E. Percoraro, L. A. O. Nunes, T. Catunda, and S. Gama, *Phys. Rev. B* **57**, 10545 (1998).
- ²⁵M. Franko and C. D. Tran, *Rev. Sci. Instrum.* **62**, 2438 (1991).
- ²⁶M. S. Baptista and C. D. Tran, *J. Phys. Chem. B* **101**, 4209 (1997).
- ²⁷M. S. Baptista and C. D. Tran, *J. Phys. Chem.* **US-99**, 12952 (1995).
- ²⁸S. M. Lima, A. C. Bento, T. Catunda, R. Lebullenger, A. C. Hernandez, M. L. Baesso, and L. C. M. Miranda, *Phys. Rev. B* **60**, 15173 (1999).
- ²⁹M. L. Baesso, J. R. D. Pereira, A. C. Bento, A. J. Palangana, A. M. Mansanares, and L. R. Evangelista, *Braz. J. Phys.* **28**, 359 (1998).
- ³⁰J. R. D. Pereira, A. J. Palangana, A. M. Mansanares, E. C. da Silva, A. C. Bento, and M. L. Baesso, *Phys. Rev. E* **61**, 5410 (2000).
- ³¹T. Higashi, T. Imasaka, and N. Ishibashi, *Anal. Chem.* **55**, 1907 (1983).
- ³²J. Shen, R. D. Lowe, and R. D. Snook, *Chem. Phys.* **165**, 385 (1992).
- ³³J. Shen, M. L. Baesso, and R. D. Snook, *J. Appl. Phys.* **75**, 3738 (1994).
- ³⁴R. Bachmann, R. E. Schawall, H. U. Thomas, R. B. Zubeck, C. N. King, H. C. Kirsh, F. J. Disalvo, T. H. Geballe, K. N. Lee, R. E. Howard, and R. L. Greene, *Rev. Sci. Instrum.* **43**, 205 (1972).
- ³⁵M. Sparks, *J. Appl. Phys.* **42**, 5029 (1971).

- ³⁶ *Polymer Handbook*, 3rd ed., edited by J. Bandrup and E. H. Immergut (Wiley, New York, 1989), p. V/61.
- ³⁷ G. K. White, S. B. Woods, and M. T. Elford, *Phys. Rev.* **112**, 111 (1958).
- ³⁸ K. Eierman, *J. Polym. Sci., Part C: Polym. Symp.* **6**, 157 (1964).
- ³⁹ I. Perepechko, *Low Temperature Properties of Polymers* (MIR Publish., Moscow, 1980). Chapters 2 and 7.
- ⁴⁰ E. A. Friedman, A. J. Ritger, and R. D. Andrews, *J. Appl. Phys.* **40**, 4243 (1969).